



Removal of Congo red and Naphthol blue black dyes from aqueous solution by adsorption on activated carbon. Characterization, kinetic and equilibrium in nonlinear models studies

Halima Setti Benammar^{a,b}, Saadia Guergazi^{a,b,*}, Soufiane Youcef^{a,b}, Leila Youcef^{a,b}

^aResearch Laboratory in Subterranean and Surface Hydraulics, Biskra University, Algeria

^bDepartment of Civil Engineering and Hydraulic, Faculty of Sciences and Technology, Biskra University, P.O. Box: 145 RP, Biskra 07000, Algeria, emails: s.guergazi@univ-biskra.dz (S. Guergazi), halimasetti.benammar@univ-biskra.dz (H.S. Benammar), soufiane.youcef@univ-biskra.dz (S. Youcef), l.youcef@univ-biskra.dz (L. Youcef)

Received 29 August 2020; Accepted 9 January 2021

ABSTRACT

The objective of our study is to test the performance of the commercial powdered activated carbon (PAC) in the elimination by adsorption of two di-azo dyes, Congo red (CR) and Naphthol blue black (NBB), were used directly without any treatment. The PAC was characterized using X-ray diffraction, Fourier transform infrared spectroscopy, Brunauer–Emmett–Teller, and the pH point of zero charges (pH_{pzc}). The adsorption studies were conducted on a batch process and under the effect of various operational parameters such as contact time, pH, and initial concentration of the tested dyes. The adsorption mechanism with nonlinear equations, such as pseudo-first-order, pseudo-second-order, intraparticle diffusion, Elovich kinetics, Langmuir, Freundlich, and Dubinin–Radushkevich isotherm was also studied. The adsorption process occurred rapidly for NBB than CR. However, the maximum adsorption capacity was obtained with CR (53.17 mg/g). The findings showed that CR and NBB's adsorption processes favor the pattern of pseudo-first-order. The maximum removal of two dyes was achieved under acidic condition. The adsorption efficiency also decreased with the initial increase in the contents of the CR and NBB. The Langmuir isotherm offered the best fit to experimental data suggesting homogeneous dispersion of adsorption sites.

Keywords: Adsorption; Congo red; Naphthol blue black; Powdered activated carbon; Kinetic; Isotherm nonlinear

1. Introduction

Water pollution is an unfavorable change in physical, chemical or biological properties, or any discharge of liquid, gaseous or solid substances into the water to create a nuisance or to make this water dangerous for use. Water pollution is mainly caused by human activities as well as natural phenomena. In this context, we find that industries represent the greatest polluters, with the textile industry generating high liquid effluent pollutants due

to the large quantities of water used in fabric processing. In this industry, wastewaters of varying composition are produced, from which colored water released during the dyeing of fabrics may be the most problematic. Since a small quantity of dye is highly visible due to its color and can cause a series of several pollution problems [1].

The textile industry generates highly polluting wastewaters and their treatment is a very serious problem due to high total dissolved solids, presence of toxic heavy metals, and dyes are chemically stable and non-degradable

* Corresponding author.

Saadia Guergazi, email: s.guergazi@univ-biskra.dz

which are aesthetically and environmentally unacceptable [2,3]. For these reasons, the textile industry has been listed as the most important source of pollution of water.

Many studies have revealed, that dyes have toxic effects, which may seriously harm the environment, like the destruction of the water system and damaging the aquatic communities. It is well acknowledged that dyes are severely harmful to human health and other living organisms. They are known to cause nausea, vomiting, skin problems like irritation, dermatitis, allergies, even reported to be carcinogenic and mutation agents in human [2–6]. In the same context a study carried out by Mittal [7] on permissible synthetic food dyes in India, pointed out several researches have been repeatedly made that artificial dyes cause serious side effects, such as hyperactivity in children as well as cancer and allergies. Therefore, the elimination of colored effluent is an absolute requirement before its discharge into the aquatic environment.

There are many processes available for the removal of dyes by conventional treatment technologies including biological and chemical oxidation, coagulation and adsorption, but they cannot be effectively used individually. Adsorption is widely acknowledged as the most promising and efficient method because of its low capital investment, simplicity of design, ease of operation, insensitivity to toxic substances and ability to remove pollutants even from diluted solutions [2–5]. Moreover, the performance is dependent on the type of carbon used and the characteristics of the wastewater. Due to its highly porous nature, activated carbon has a much larger surface area, and hence has a higher capacity in terms of the adsorption [3].

It is important to note that the textile dyes have been classified according to their chemical structure (azo dyes, nitro dyes, indigo dyes, anthraquinone dyes, phthalen dyes, triphenylmethyl dyes, nitrated dyes, etc.) [8]. Azo dyes are the largest class of synthetic dyes that are characterized by the presence of one or more azo bonds (R1-N=N-R2). Congo red (Direct red 28) and Naphthol blue black (Amido black 10B) are among the widely known azo colorants used in the textile industry. While the adsorption using different adsorbent materials can be used to eliminate these two dyes, their negative effects and toxicity remain of concern as mentioned by many studies [5,9,10]. In this context, the activated carbon may serve as an ideal adsorbent because of its low-cost. It has relatively large specific surface area, excellent physical and chemical stability. In addition, the activated carbons are not only capable of sequestering contaminants with varying molecular size, but also have considerably high adsorption capacities, and other advantageous structural and surface properties [2,3].

Therefore, the present work explores the performance of the commercial powder activated carbon in the elimination

of the two di-azo dyes, Congo red (CR) and Naphthol blue black (NBB). To realize our goals and to highlight the treatment performances of the powdered activated carbon, various operational parameters like, the effect of the agitation time, pH, the variation of the mass of adsorbent will be studied. In addition, the kinetics of adsorption (effect of the variation in contact time) and the variation in the mass of the adsorbent will be crowned by the application of the different models.

2. Materials and methods

2.1. Adsorbate

In this research work, the used dyes of CR and NBB have obtained from Sigma-Aldrich and used without any purification. The location for the company are respectively product by India and USA. These two colorants are anionic dyes that are a part of the class of azo are anionic dyes. The CR characterized by a dye content $\geq 35\%$, molecular formula: $C_{32}H_{22}N_6O_6S_2Na_2$ and molecular weight: equal to 696.66 g/mol. The NBB marked by 80% dye content, molecular formula: $C_{22}H_{14}N_6Na_2O_9S_2$ and molecular weight equal to 616.49 g/mol. Their molecular structures are schematically presented in (Fig. 1). A stock solution of the studied dyes (CR and NBB) was prepared by dissolving 1 g of dye in distilled water and then making the volume up to 1,000 mL with water, then stored in a volumetric flask. Samples of different concentrations of dyes were prepared from the stock solution by dilution. The calibration curves of CR and NBB solutions were obtained by measuring the absorbance of these samples at the maximum absorbance wavelength of $\lambda_{max} = 500$ nm for CR and $\lambda_{max} = 618$ nm for NBB using a UV-Vis spectrophotometer (Optizen).

2.2. Adsorbent

The studied powdered activated carbon (PAC) has been provided by Riedel-de Haën chemicals laboratory and the company product by Germany. This adsorbent was directly applied without further grinding and sieving. PAC's structure was characterized by X-ray diffraction (XRD) using the pert high score plus of a PANalytical X. Over a range of 2θ and scanning rate were 2° – 70° and 2°min^{-1} , respectively. The PAC surface functional groups are studied using Fourier transform infrared (FTIR) spectroscopy (Shimadzu IRAffinity-1S), the manufacturer location for the company product by Japan. FTIR spectrums were recorded with KBr disk method in wavenumber range of 400 – $4,000$ cm^{-1} . Nitrogen adsorption-desorption isotherms were obtained by Micromeritics ASAP 2010 V5.00 instrument giving the textural characteristics of PAC samples at 77.30 K, the manufacturer location for

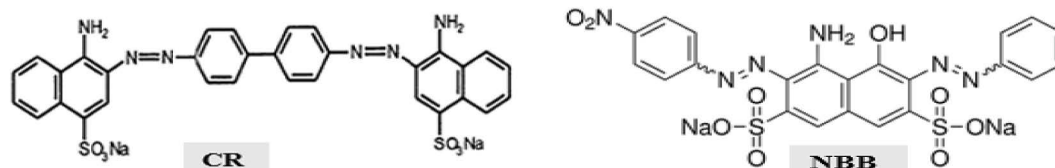


Fig. 1. Structure of CR and NBB.

the company product by USA. Furthermore, the point of zero charge (pH_{PZC}) was determined by a classical method [11] that consists of preparing 50 mL NaCl (0.01 M) solutions and changing their pH to correct values from 2 to 11 by adding NaOH or HCl (0.1 M). Then 0.5 g of adsorbent was applied to each solution. Before determining the final pH (pH_{final}), the suspensions were stirred at room temperature for 24 h. The pH_{PZC} was determined using

the curve of $\text{pH}_{\text{final}} - \text{pH}_{\text{initial}} = f(\text{pH}_{\text{initial}})$. The obtained results are presented in Figs. 2a–e, respectively.

2.3. Description of adsorption tests

The elimination trials of CR and NBB, on PAC were performed in batch experiments at room temperature, on a magnetic stirrer by contacting a synthetic solution

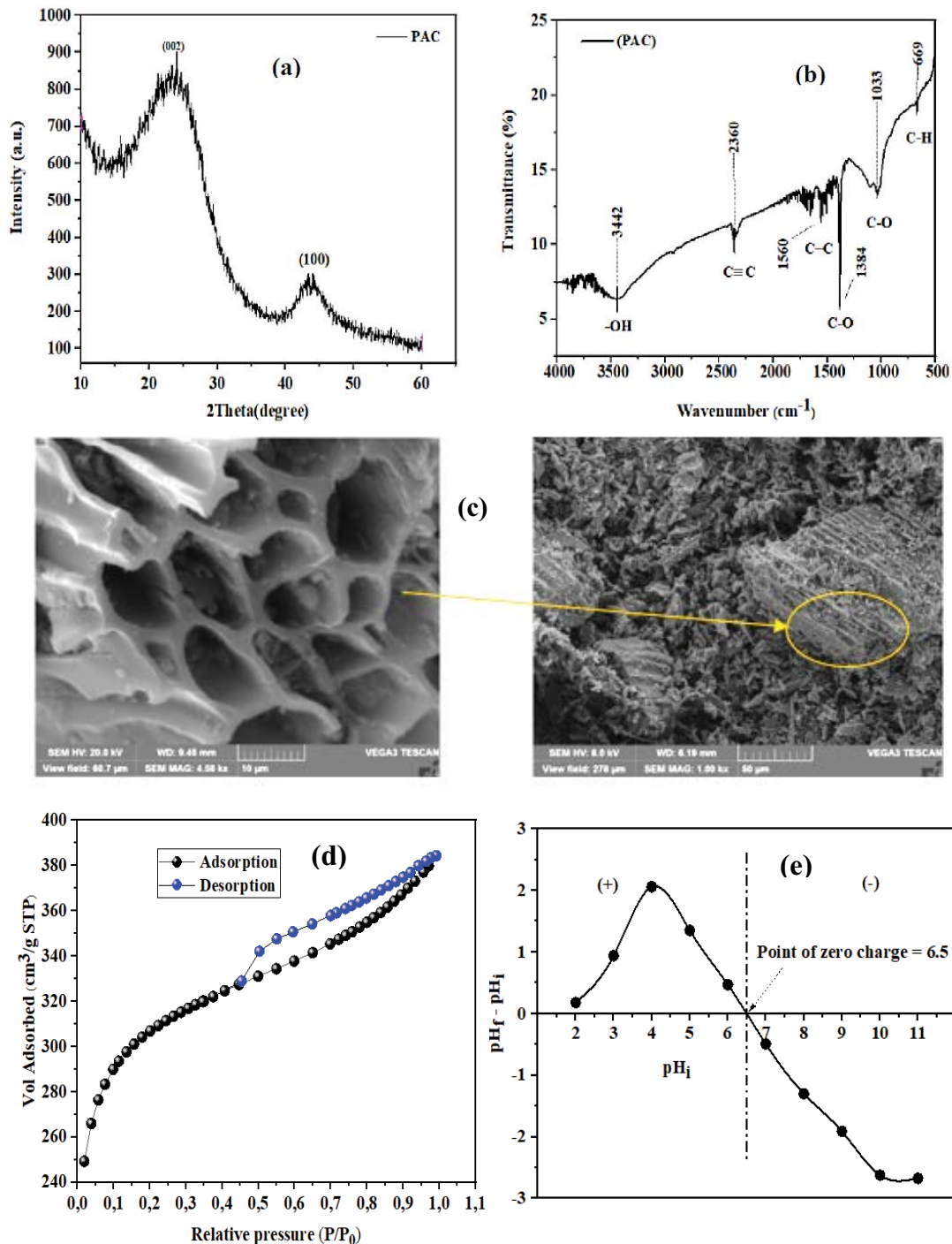


Fig. 2. Characterization of PAC sample: (a) XRD patterns, (b) FTIR spectra, (c) scanning electron microscopy (SEM) micrographs, (d) nitrogen adsorption and desorption isotherms (at 77.30 K, equilibration interval: 5 s), and (e) pH point of zero charges of PAC sample.

of these two dyes (30 mg/L of CR and 20 mg/L for NBB), with a constant mass of activated carbon powder (0.5 g). Each sample is filtered by vacuum using 0.45 μm of membrane porosity. For each filtered sample was measured the residual content of CR and NBB by a UV-Vis spectrophotometer at λ_{max} = 500 nm for CR and λ_{max} = 618 nm for NBB. Our tests were conducted in distilled water, without any pH adjustment. Different parameters were tested for examining the impact of the elimination of CR and NBB on powdered activated carbon: the stirring time (2 min–5 h), the pH ranged from 2 to 12 with the successive adjustment of the pH, by adding hydrochloric acid to obtain the acid pH and sodium hydroxide (NaOH) to obtain the basic (alkaline) pH. The solution pH was kept constant during the agitation (equilibrium time). The effects of the variation of the initial concentration of NBB and CR were also studied.

Our study was also crowned by the application of various nonlinear models that are very useful in the field of adsorption, such as pseudo-first-order [12], pseudo-second-order [13], Elovich [14] and intraparticle diffusion models [15] for the kinetics study. Langmuir [16], Freundlich [17], and Dubinin–Radushkevich [18] for isotherms study. The formulas of the above-mentioned models nonlinear are generally expressed by Eqs. (1)–(7):

The pseudo-first-order model is expressed as:

$$q_t = q_e \left(1 - e^{(-k_1 t)}\right) \quad (1)$$

The pseudo-second-order is represented by the following equation:

$$q_t = \frac{q_e^2 k_2 t}{1 + q_e k_2 t} \quad (2)$$

The Elovich model is defined as follows:

$$q_t = \frac{1}{\beta} \times \ln(1 + \alpha \times \beta \times t) \quad (3)$$

The intraparticle diffusion model is expressed by the following equation:

$$q_t = K_p t^{1/2} + C \quad (4)$$

The Langmuir model is illustrated by the following equation:

$$q_e = \frac{Q_{\max}^0 k_L C_e}{1 + k_L C_e} \quad (5)$$

The Freundlich model is described by the following equation:

$$q_e = k_F C_e^n \quad (6)$$

The Dubinin–Radushkevich model is in the following equation:

$$q_e = q_{DR} e^{-K_{DR} \epsilon^2} \quad (7)$$

$$E = \frac{1}{\sqrt{2K_{DR}}} \quad (8)$$

2.4. Error function analysis

To determine the suitability of a model equation to experimental results, an evaluation of the error function is normally needed. The best-fitting sorption kinetic and equilibrium isotherm models were validated using three different statistical error functions namely coefficient of determination (R^2), adjusted coefficient of determination (R_{adj}^2), and Chi-square (χ^2). Noting that, if the q_e experimental values are similar to the q_e model values, χ^2 is close to zero. A high χ^2 value suggests a strong disparity between the values of the experimental and the measured model.

The equations of all the employed error functions are as follows [Eqs. (9)–(11)]:

$$R^2 = 1 - \frac{\sum (q_{e,exp} - q_{e,cal})^2}{\sum (q_{e,exp} - q_{e,mean})^2} \quad (9)$$

$$R_{adj}^2 = 1 - \left[(1 - R^2) \times \left(\frac{n - 1}{n - p - 1} \right) \right] \quad (10)$$

$$\chi^2 = \sum_{i=1}^n \frac{(q_{e,exp} - q_{e,cal})^2}{q_{e,cal}} \quad (11)$$

where q_e mean is the mean of the $q_{e,exp}$ values; n is the number of experiments, and p is the number of parameters in the selective model.

3. Results and discussion

3.1. Characterization of PAC

The different characteristics of the tested adsorbents are grouped in Fig. 2. XRD patterns of PAC, Fig. 2a show the presence of broad peaks around 23° and 43°, attributed to Bragg reflections (002) and (100) of amorphous carbon. They signify the partially graphitic structure of the activated carbon sample [19] while the presence of similar peaks signifies a high degree of disorder and typical of carbonaceous materials. Other researchers working on produced activated carbon from agricultural wastes have obtained similar results [20]. Fig. 2b reveals the qualitative details about the functional groups present on the PAC surface. The strong bands at about 3,442 cm⁻¹ were related to stretching hydroxyl group (–OH) vibrations in alcohol groups, phenol groups or adsorbed water groups. The peaks at about 2,360 cm⁻¹ suggest the presence of a triple bond carbon–carbon (C≡C) in disubstituted alkynes [21,22].

Further, bands appearing between 1,600 and 1,560 cm⁻¹ were ascribed to C–C vibrations in aromatic rings. The characteristics of carboxylic and lactonic groups (C–O) groups

were endorsed by the presence of peaks at around $1,384\text{ cm}^{-1}$ [21,23]. The C–O stretching vibrations of cellulose structure are responsible for the sharp bands at around $1,033\text{ cm}^{-1}$. Finally, the bands observed between $1,000$ and 500 cm^{-1} were due to the out-of-plane deformation mode of C–H for alkene aromatic rings.

The results of the PAC scanning electron microscopy (SEM) showed a porous surface structure as displayed in Fig. 2c while the availability of pores and the internal surface is required for an effective adsorbent. The presence of large pores permits greatly the adsorption of the CR and NBB to the pores. Besides, in the presence of large pores, there is a good chance of the CR and NBB to be adsorbed to the pores.

The presence of carbon in the sample is further illustrated by the energy-dispersive X-ray micrograph showing the presence of C (92.54%) and O (7.17%), and small amounts of Ca (0.10%) and Na (0.19%). Because of these facts, it can be concluded that the PAC presents an adequate morphology for CR and NBB adsorption [22].

The specific surface analysis of this adsorbent was found to be $1,147.48\text{ m}^2/\text{g}$. As shown in Fig. 2d, the PAC adsorption–desorption isotherms belong to the form I isotherm typical of activated carbons as described by the International Union of Pure and Applied Chemistry (IUPAC). The type I isotherm demonstrates a narrow pore size distribution (average pore diameter was found to be equivalent to $1.71 < 2\text{ nm}$) with a small external surface area [24]. This is well consistent with the textural properties of the PAC sample. Micropore (S_{Micro}) and external (S_{Ext}) surface areas ranged from 840.61 and $306.87\text{ m}^2/\text{g}$, respectively.

In general, the hysteresis loop is present in the adsorption/desorption isotherms (Fig. 2d). Hysteresis appearing

in the multilayer range of physical adsorption at the pressure rate (P/P_0) between 0.4 and 0.8 which is related to the presence of mesoporous in the materials, that is associated with narrow slit-like pores [25].

pH point of zero charges (pH_{pZC}) was determined by curve in Fig. 2e. It was found that pH_{pZC} of PAC was 6.5. The pH_{pZC} of PAC refers to the pH of the solution at which its net surface charge is zero. When the pH of the solution $>\text{pH}_{\text{pZC}}$, the adsorbent reacts as a negative surface and as a positive surface when the solution pH is $<\text{pH}_{\text{pZC}}$ [26].

3.2. Adsorption kinetics studies

3.2.1. Effect of stirring time

The effect of the contact time on the adsorption of two tested dyes, namely NBB and CR are illustrated in Fig. 3a. From these results, we can say that the adsorption on powdered activated carbon, of NBB and CR dyes, is effectively evaluated by increasing in the contact time. The maximum retention is achieved after 45 min of contact time for NBB and 180 min for the CR. The maximum amount adsorbed q_t (mg/g) was 29.33 mg/g (percentage removal % = 73.33) and 53.17 mg/g (percentage removal % = 88.64) for NBB and CR respectively. After this optimum adsorption an almost equal equilibrium appeared, proves the saturation of the active sites of the adsorbent. Whereas, the adsorption phenomenon of NBB and CR on activated carbon was quite rapid because not less than 60% of the dye present in the solution was sequestered on the surface of the adsorbent support after 10 min. This could be due to the specific surface area of the PAC, which is quite large (of the order of $1,147.48\text{ m}^2/\text{g}$). In the same way,

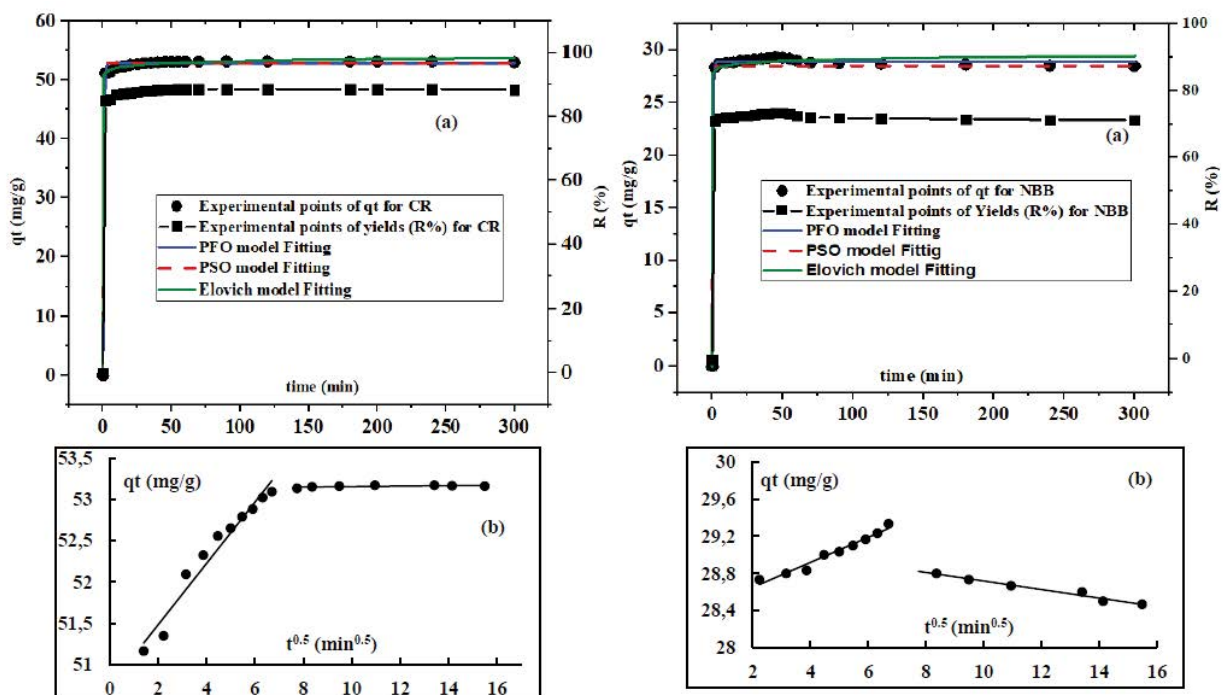


Fig. 3. Effect of contact time on the adsorption of PAC towards CR and NBB dyes (experimental conditions: co. of CR = 30 mg/L , co. of NBB = 20 mg/L , PAC = 0.50 g).

the dose of the adsorbent in solution is quite sufficient, so that makes it possible to ensure an equivalent number of adsorption sites for the tested dyes. In addition, the high affinity of CR and NBB with respect to PAC.

It is important to note that our results could be confirmed by Somasekhara et al. [11], during the elimination of CR by adsorption on a biomaterial, they recorded that the equilibrium attains approximately at 1, 1.5, 2 and 2.5 h for dye concentrations 25, 50, 75 and 100 mg/L, respectively. Hu et al. [27] and Somasekhara Reddy [28] studied and reported that the adsorption equilibrium of CR on cattail root and tamarind fruit shell took 3 h and 7 h respectively. Venkat and Vijay Babu [29], registered that the kinetics of adsorption on sawdust of CR is a gradual process with quasi-equilibrium attained in 4 h. Ghasemian and Palizban [30] findings after the comparison of the azo dye adsorption on activated carbon (AC) and silicon carbide nanoparticles (SiCNP) loaded on AC revealed that SiCNP-AC had a reasonably good adsorption potential of 78.74 mg/g for methyl orange and 40.16 mg/g for CR. Therefore, they showed that equilibrium was achieved after 50 min and assumed that the equilibrium being due to the saturation of the active site, at which time further adsorption cannot take place.

As stated by Akram et al. [9], during the removal of the azo dye (Acid red 18), from aqueous solution by adsorption onto activated carbon prepared from almond shell, registered the maximum adsorption capacity (44 mg/g) that occurred at 2 h contact time, and 42.4% of the adsorption capacity was reached for 60 min of the equilibrium time. Meantime, Vasuki and Karthika [4] found the adsorption efficiency of coconut shell (CSC) and palmyra fruit nutshell (PFSC) for Naphthol blue black-B dye for at an equilibrium time 60 min, the percentage of removal of 22.4% and 40.11% respectively. Thus, the efficiency of adsorption by palmyra carbon is twice that of coconut carbon. A study conducted by Karthika and Vasuki [6], on the adsorptive removal of synthetic dye effluent using sago waste as low-cost adsorbent, indicated that 79.2% of Naphthol blue black-B dye removed at 40 min.

According to other studies findings by Munagapati et al. [8]; Kaur and Kaur, [10], Ghasemian and Palizban, [30] and Yadav et al. [31], the equilibrium time is linked to the initial concentration of the dye; it increases with increasing concentrations and vice versa. Since the stirring speed is constant, the diffusion of the dye molecules towards the active surface of the adsorbent material is affected by the initial concentration of the dye. As a result, the rise in dye concentration accelerates the latter’s diffusion due to the increase in the concentration gradient’s attraction powers.

3.2.2. Adsorption kinetic study

The pseudo-first-order, pseudo-second-order, Elovich, and intraparticle diffusion models [Eqs. (1)–(4)] were used to describe the adsorption rate of CR and NBB onto PAC. The results of the cited models are presented in the curve of Figs. 3a and b and in Table 1.

- As seen in Fig. 3a and Table 1, very good correlation coefficients that were obtained were close to unity for the four tested models, which indicates the simultaneous

Table 1
Kinetic parameters for adsorption of CR and NBB onto PAC

Models	CR	NBB
Pseudo-first-order		
$q_{e,exp}$ mg/g	53.95	29.33
$q_{e,cal}$ mg/g	52.85	28.91
k_1 , 1/m	1.71	1.95
R^2_{adj}	0.998	0.998
R^2	0.998	0.998
χ^2	0.217	0.068
Pseudo-second-order		
$q_{e,exp}$ mg/g	53.95	29.33
$q_{e,cal}$ mg/g	52.76	28.50
k_2 , 1/m	8.89	1.97
R^2_{adj}	0.997	0.994
R^2	0.997	0.994
χ^2	0.36	0.25
Elovich		
β , mg/g	1.972	3.67
α , mg/g min	1.85	8.89
R^2_{adj}	0.999	0.995
R^2	0.999	0.995
χ^2	0.0865	0.210
Intraparticle diffusion		
First stage		
K_p , mg/g/m ^{1/2}	0.372	0.134
C , mg/g	50.734	28.38
R^2	0.960	0.967
Second stage		
K_p , mg/g/m ^{1/2}	0.003	0.046
C , mg/g	53.13	29.17
R^2	0.94	0.97

occurrence of physical diffusion and chemical adsorption between respectively CR and NBB on PAC.

- The mean χ^2 values of pseudo-first-order, pseudo-second-order, and Elovich nonlinear kinetic model varied from 0.086–0.36 and 0.069–0.20, respectively for NBB and CR. In this case, for CR, the Elovich model represents the experimental data better as compared to other pseudo-first-order and pseudo-second-order. However, the pseudo-first-order for the NBB was better than the pseudo-second-order and Elovich.
- Our results show at first that, the q_p experimental (53.17 mg/g) for CR and (29.33 mg/g) for NBB was closer to the q_p calculated values for the pseudo-first-order model (CR = 52.85 mg/g and NBB = 28.90 mg/g) than the value of the pseudo-second-order (52.76 and 28.86 mg/g), respectively for CR and NBB. On the other hand, a higher R^2_{adj} (0.998), R^2 values (0.998), and lower χ^2 (0.068 and 0.217) respectively for NBB and CR

confirmed that the adsorption process was best described by the pseudo-first-order.

- The diffusion phenomenon was demonstrated by carrying the quantity adsorbed of CR and NBB (q_t (mg/g)) as a function of $t^{1/2}$ as shown in Fig. 3b and Table 1.
- According to Weber and Morris [15], if the curve $q_t = f(t^{1/2})$ does not pass through the origin, "C" will be different from zero. This proves the existence of the effect of the diffusion boundary layer (that is, the adhesion to the surface of the external diffusion and the adsorbate to the external surface of the adsorbent). Thus, intraparticle diffusion is not the only controlling stage in adsorption and the rate of adsorption is controlled by another mechanism.

In this context, the obtained lines (Fig. 3b) do not pass through the origin and the double linearity is well observed on the curve $q_t = f(t^{1/2})$ for the powdered activated carbon tested for CR as well as for NBB. Table 1 presents the parameters of the intraparticle scattering model. The recorded values of the diffusion rate constants during the first step were higher than the second step, which indicates that the speed of the first phase of the kinetics is fast.

3.2.3. Determination of the effect of initial pH

The pH of the solution ($\text{pH}_{\text{Solution}}$) plays a very important role in the degradation of chemical pollutants because it modifies their physical properties by ionization of the functional groups. However, certain dyes, in particular the colored indicators, change color depending on the pH of the medium. To reach our objective, the tests were carried out in the presence of a constant concentration of NBB (20 mg/L), CR (30 mg/L) and 0.5 g/L of PAC. While varying the pH of the medium in a range from 2 to 12. The $\text{pH}_{\text{Solution}}$ is kept constant during the 120 min and 45 min of agitation (equilibrium time) for the CR and the NBB respectively. At equilibrium, the obtained results are presented in Fig. 4.

Fig. 4 shows that the adsorption of NBB and CR dyes depends on the $\text{pH}_{\text{Solution}}$. In the $\text{pH}_{\text{Solution}}$ ranging from 2 to 4, a high percentage of elimination of the two dyes was observed (>90% and >80%, respectively for CR and NBB at $\text{pH}_{\text{Solution}}$). The acid medium was favorable to the adsorption process of NBB and CR.

- The adsorption capacity is high for two tested dyes at $\text{pH}_{\text{Solution}} < \text{pH}_{\text{PZC}}$. Because, this medium (acid) leads to an increase in the concentration of H^+ ions in solution, which gives the material a positive surface charge. Strong electrostatics attractions appear between the positive surface sites of the adsorbent and the anionic charges of the molecules of CR and NBB dyes, hence the high adsorption capacity which greatly exceeded 50%.
- Deprotonation occurs at $\text{pH}_{\text{Solution}} > \text{pH}_{\text{PZC}}$; hence, diffusion and adsorption decrease, which automatically leads to a decrease in the removal rate of the discoloration.

Therefore, our observed results were consistent with previous studies [9,10,32] that were conducted on the effect of $\text{pH}_{\text{Solution}}$ during the removal of dyes regardless of the type of adsorbent material.

As aforementioned, a study on the influence of $\text{pH}_{\text{Solution}}$ on the chemical treatment of two dyes was tested, and the coloring of NBB solutions remained stable regardless of the variation in $\text{pH}_{\text{Solution}}$. Though the CR observed with the variation of the $\text{pH}_{\text{Solution}}$ from 2 to 10, and the solution changes from red to dark blue. These findings are compatible with the study of Ait Ahsaine et al. [32], who suggested that the CR diazo dye (free $\text{pH}_{\text{Solution}} = 7$) changes from red to dark blue, as well as at $\text{pH}_{\text{Solution}}$ greater than 10.

3.2.4. Determination of the effect of the initial concentration of CR and NBB with a fixed dose of PAC

In order to study the effect of the initial concentration of CR and NBB, batch experiments have been conducted at a fixed PAC dose of 0.5 g/L by increasing the concentration of CR and NBB from 10 to 100 mg/L. The CR and NBB residual contents of the treated samples were measured after 45 min and 180 min of contact time for NBB and CR respectively. All of our results are presented on the curves of Figs. 4a and b respectively for removal percentages of CR, NBB, and non-linear isotherms equations.

The results of Fig. 4a display that the concentration of dye has a definite effect on the rate of discoloration (elimination of color). As, the higher the pollutant concentration, the slower the discoloration, which is expected. After 45 min and 180 min of treatment, the discoloration is noted with PAC at a rate of 82.70%–88.64% and 60.72%–73.33% respectively for concentrations 10–30 mg/L for CR and 10–25 mg/L for NBB.

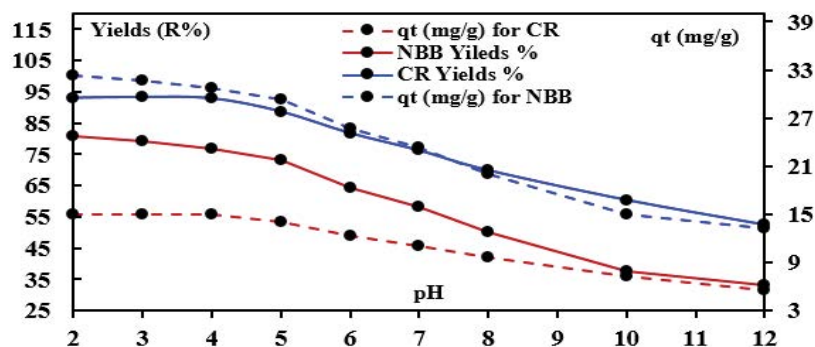


Fig. 4. Effect of $\text{pH}_{\text{Solution}}$ on the removal of CR and NBB by adsorption on PAC ([CR] = 30 mg/L; [NBB] = 20 mg/L; PAC = 0.5 g).

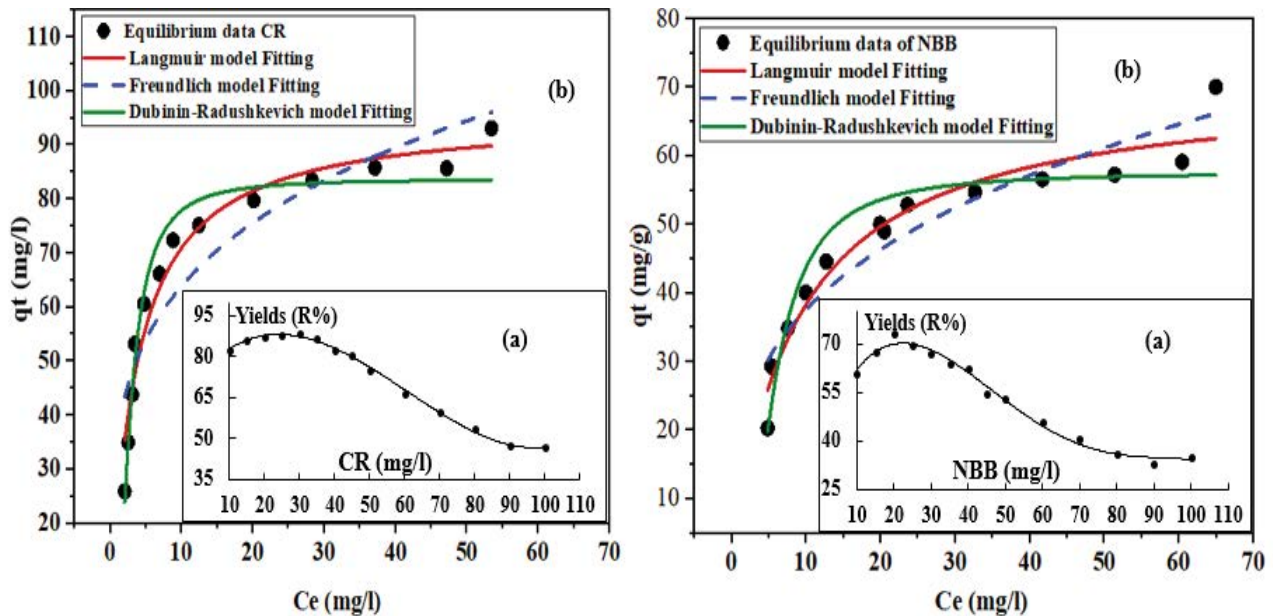


Fig. 5. Effect of initial dye concentration on adsorption for CR and NBB (a) and isotherm for adsorption of CR and NBB onto PAC (b).

For concentrations higher than 30 and 25 mg/L until 100 mg/L, there is a less remarkable decrease in the efficiency of the process in both for CR and that of NBB. In this case, a low concentration of dye can be noticed; there will be unoccupied binding sites on the surface of the adsorbent. The initial concentration of dye increased which may cause insufficient sites for the dye molecules to adsorb 0.5 g/L of PAC and so, the efficiency of dye removal decreased. Similar research on the removal of Acid red 18 (azo dye) from aqueous solution by adsorption on activated charcoal prepared from the almond shell was observed by Akram et al. [9].

However, our findings are in agreement with the all previous studies of [6,11,29,31], which underlined, that the initial concentration of the dye in the liquid phase significantly affects the adsorption process. The impact depends on several parameters, such as the nature of the dye and the liquid medium, the presence or the availability of the functional groups on the surface of the adsorbent, and the adsorption capacity of the dye. In most cases, the increase in the initial concentration of dye results in an increase for dye adsorbed per unit mass of adsorbent until a plateau is reached or when an overall decrease in efficiency elimination appears.

3.2.5. Adsorption isotherm study

The adsorption isotherm is to investigate the relationship between the amount of dye adsorbed at constant temperature and its concentration in equilibrium solution. Many isotherms describe sorption such as Langmuir, Freundlich, Brunauer–Emmett–Teller, Toth, Temkin, Redlich–Peterson, Sips, Frumkin, Harkins–Jura, Halsey, Henderson, and Dubinin–Radushkevich. According to the models of Langmuir [16], Freundlich [17], and Dubinin–Radushkevich [18], the isotherms in their nonlinear forms

were chosen in this study to interpret our experimental data. All the equations of the mentioned isotherm models are expressed [Eqs. (5)–(7)].

All isotherm models are graphically demonstrated in Figs. 5a and b respectively for CR and NBB with good correlation ($R_{adj}^2 > 0.80 \approx 1$). It indicates the high affinity of PAC adsorbent toward CR and NBB in solution, and the isotherm parameters are listed in Table 2. From all our results, we can say:

- The Langmuir isotherm model (R_{adj}^2 0.993) is more appropriate as compared to R_{adj}^2 value of Freundlich and Dubinin–Radushkevich. The Langmuir isotherm model agrees to the formation of monolayer adsorption in between CR and NBB on the surface of PAC. The maximum adsorption capacity ($q_{max} = 70.90$ mg/g for NBB and 95.70 mg/g for CR) is higher than Dubinin–Radushkevich has shown in Table 2. The calculated R_L values were 0.075–0.46 and 0.034–0.26 respectively for NBB and CR, this range is between 0 and 1, which indicated, that the adsorptions of both tested dyes were favorable for the PAC.
- For the Freundlich isotherm model, it was observed that the value of n is 0.243 and 0.302 respectively for CR and NBB, which is less than 1. This parameter shows favorable adsorption of adsorbate and adsorbent. In the same way, the values of k_F (Freundlich constant) greater than 1, indicate that the adsorption is favorable and physical.
- For the Dubinin–Radushkevich model, the adsorption energy on PAC of the two tested dyes at a temperature of $T = 293 \pm 1$ K, were 0.310 and 0.605 kJ/mol respectively for the NBB and RC. These values indicated the predominance of physical adsorption reactions, because ($E < 8$ kJ/mol) suggested the physical nature of the adsorption interactions. Once again, we confirmed what was obtained with the Freundlich model ($k_F > 1$).

Table 2
Isotherms parameters for adsorption of CR and NBB onto PAC

Isotherms	CR	NBB
Langmuir		
Q_{\max}^0 , mg/g	95.70	70.64
k_L , l/mg	0.2864	0.120
R_{adj}^2	0.993	0.936
R^2	0.956	0.942
χ^2	21.466	11.691
Freundlich		
k_F , ((mg/g)/(mg/L)) ⁿ	36.515	18.794
n	0.2430	0.302
R_{adj}^2	0.833	0.886
R^2	0.85	0.896
χ^2	75.13	20.89
Dubinin–Radushkevich		
q_{DR} , mg/g	83.706	57.623
K_{DR} , mol ² /kJ ²	1.3645×10^{-6}	5.188×10^{-6}
R_{adj}^2	0.958	0.865
R^2	0.961	0.877
χ^2	18.988	24.712
E , kJ/mol	0.605	0.310

Several other studies reported, if the value of E is less than 8 kJ/mol the adsorption follows physical sorption. If the value of E is between 8–16 kJ/mol, the adsorption showing chemical ion-exchange and above 40 kJ/mol presenting chemisorption mechanism [20,26].

4. Conclusion

The current study shows that FTIR results confirmed the existence of hydroxyl and carboxyl functional groups in powdered activated carbon. The Brunauer–Emmett–Teller results show that the adsorbant is a microporous material. The microporous character of powdered activated carbon was attributed to the activation process during the synthesis process.

Our findings suggest that the powdered activated carbon is more suitable adsorbent for Congo red removal than the Naphthol blue black in batch experiments. Moreover, we pointed out that:

- The elimination of Congo red and Naphthol blue black recorded very good efficiency accompanied by a relatively fast equilibrium time for Naphthol blue black (45 min) in comparison with that of Congo red (180 min). Kinetic studies revealed that, the adsorption of both dyes onto powdered activated carbon was best described by the pseudo-first-order model.
- The adsorption was shown to depend on the solution pH and the optimum pH value for the better adsorption was found in the interval from 2.0 to 4.0 ($\text{pH}_{\text{Solution}} \ll \text{pH}_{\text{PZC}}$).
- The adsorption efficiency also decreased with an

increase in the concentration of Naphthol blue black and Congo red.

- The adsorption isotherms showed that the adsorption of Naphthol blue black and Congo red dyes onto PAC fits well to the Langmuir.

To sum, this study permitted to demonstrate that the powdered activated carbon has a remarkable effect on the adsorption of anionic di-azo dyes and has a good application prospect in the treatment of wastewater and dye pollution.

Acknowledgments

This work was supported by the Research Laboratory in Subterranean and Surface Hydraulics (LARHYSS), of Biskra University, and the General direction of Scientific Research and Technological Development of the Ministry of Higher Education and Scientific Research- Algeria.

Symbols

q_e	–	Amounts of dye adsorbed at equilibrium, mg/g
q_t	–	Amounts of dye adsorbed at time t , min
k_1	–	Rate constant for the pseudo-first-order, min ⁻¹
k_2	–	Rate constant for pseudo-second-order, g/min mg
α	–	Initial sorption rate, mg/g/min
β	–	Desorption constant (gm/g) related to the extent of surface coverage and activation energy for chemisorption
C	–	Constant related to the thickness of the boundary layer, mg/g
K_p	–	Intraparticle diffusion rate constant, mg/g min ^{1/2}
Q_{\max}^0	–	Maximum monolayer adsorption capacity of the adsorbant, mg/g
C_e	–	Equilibrium concentration of dye solution, mg/L
k_L	–	Langmuir constant, L/mg
C_0	–	Initial concentration of dye solution, mg/L
k_F	–	Freundlich constant, (mg/g)/(mg/L) ⁿ
n	–	Dimensionless Freundlich intensity parameter
q_{DR}	–	Maximum sorption capacity, mg/g
K_{DR}	–	Constant related to the mean sorption energy, mol ² /kJ ²
ε	–	Polanyi potential
E	–	Mean adsorption energy, kJ/mol

References

- [1] S. Soni, P.K. Bajpai, J. Mittal, C. Arora, Utilisation of cobalt doped iron based MOF for enhanced removal and recovery of methylene blue dye from waste water, *J. Mol. Liq.*, 314 (2020) 113642, <https://doi.org/10.1016/j.molliq.2020.113642>.
- [2] V. Kumar, P. Saharan, A.K. Sharma, A. Umar, I. Kaushal, A. Mittal, Y. Al-Hadeethi, B. Rashad, Silver doped manganese oxide-carbon nanotube nanocomposite for enhanced dye-sequestration: isotherm studies and RSM modelling approach, *Ceram. Int.*, 46 (2020) 10309–10319.
- [3] A. Mittal, J. Mittal, Chapter 11 – Hen Feather: A Remarkable Adsorbent for Dye Removal, S.K. Sharma, Ed., *Green Chemistry for Dyes Removal from Wastewater: Research Trends and Applications*, Scrivener Publishing LLC, USA, 2015, pp. 409–457.
- [4] M. Vasuki, M. Karthika, Adsorption characteristic of Naphthol blue black-B on activated carbon derived from coconut shell and palmyra fruit nut shell – a comparative study, *Shanlax Int. J. Arts Sci. Humanities*, 4 (2017) 336–338.

- [5] X. Wang, C. Jiang, B. Hou, Y. Wang, C. Hao, J. Wu, Carbon composite lignin-based adsorbents for the adsorption of dyes, *Chemosphere*, 206 (2018) 587–596.
- [6] M. Karthika, M. Vasuki, Adsorptive removal of synthetic dye effluent using sago waste as low-cost adsorbent, *Int. J. Waste Resour.*, 8 (2018) 344, doi: 10.4172/2252-5211.1000344
- [7] J. Mittal, Permissible synthetic food dyes in India, *Resonance – Int. J. Sci. Educ.*, 25 (2020) 567–577.
- [8] V.S. Munagapati, V. Yarramuth, Y. Kima, K.M. Lee, D.-S. Kim, Removal of anionic dyes (Reactive Black 5 and Congo red) from aqueous solutions using Banana Peel Powder as an adsorbent, *Ecotoxicol. Environ. Saf.*, 148 (2018) 601–607.
- [9] A. Akram, A.N. Chaleshtori, F.M. Meghaddam, M.M. Sadeghi, R.R. Rahimi, S. Hemati, A.A. Ahmadi, Removal of Acid red 18 (Azo-dye) from aqueous solution by adsorption onto activated charcoal prepared from almond shell, *J. Environ. Sci. Manage.*, 20 (2017) 9–16.
- [10] R. Kaur, H. Kaur, Adsorptive removal of Amido Black 10B from aqueous solution using stem carbon of *Ricinus communis* as adsorbent, *Asian J. Chem.*, 31 (2019) 1071–1076.
- [11] R.M.C. Somasekhara, L. Sivaramakrishna, R.A. Varada, The use of an agricultural waste material, Jujuba seeds for the removal of anionic dye (Congo red) from aqueous medium, *J. Hazard. Mater.*, 203 (2012) 118–127.
- [12] S. Lagergren, About the theory of so-called adsorption of soluble substances, *Kongl. Vetensk. Acad. Handl.*, 24 (1898) 1–39.
- [13] Y.S. Ho, G. McKay, Pseudo-second order model for sorption processes, *Process Biochem.*, 34 (1999) 451–465.
- [14] F.C. Wu, R.L. Tseng, R.S. Juang, Characteristics of Elovich equation used for the analysis of adsorption kinetics in dye-chitosan systems, *Chem. Eng. J.*, 150 (2009) 366–373.
- [15] W.J. Weber, J.C. Morris, Kinetics of adsorption on carbon, from solution, *J. Sanit. Eng. Div.*, 89 (1963) 31–60.
- [16] I. Langmuir, The adsorption of gases on plane surfaces of glass, mica and platinum, *J. Am. Chem. Soc.*, 40 (1918) 1361–1403.
- [17] H.M.F. Freundlich, Über die adsorption in Lösungen, *Z. Phys. Chem.*, 57 (1906) 385–470.
- [18] M.M. Dubinin, L.V. Radushkevich, Equation of the characteristic curve of activated charcoal, *Proc. Acad. Sci. Phys. Chem. Sect. USSR*, 55 (1974) 331–333.
- [19] M. Zbair, K. Ainassaari, A. Drif, S. Ojala, M. Bottlinger, M. Pirlä, R.L. Keiski, M. Bensite, R. Brahmi, Toward new benchmark adsorbents: preparation and characterization of activated carbon from argan nut shell for bisphenol A removal, *Environ. Sci. Pollut. Res.*, 25 (2018) 1869–1882.
- [20] E. Vunain, D. Kenneth, T. Biswick, Synthesis and characterization of low-cost activated carbon prepared from Malawian baobab fruit shells by H_3PO_4 activation for removal of Cu(II) ions: equilibrium and kinetics studies, *Appl. Water Sci.*, 7 (2017) 4301–4319.
- [21] M.T. Vu, H.P. Chao, T. Van Trinh, T.T. Le, C.C. Lin, H.N. Tran, Removal of ammonium from groundwater using NaOH-treated activated carbon derived from corncob wastes: batch and column experiments, *J. Cleaner Prod.*, 180 (2018) 560–570.
- [22] H.N. Tran, C.-K. Lee, T.V. Nguyen, H.-P. Chao, Saccharide-derived microporous spherical biochar prepared from hydrothermal carbonization and different pyrolysis temperatures: synthesis, characterization, and application in water treatment, *Environ. Technol.*, 39 (2018) 2747–2760.
- [23] S.M. Yakout, G. Sharaf El-Deen, Characterization of activated carbon prepared by phosphoric acid activation of olive stones, *Arabian J. Chem.*, 9 (2016) S1155–S1162.
- [24] H.N. Tran, S.J. You, T.V. Nguyen, H.P. Chao, Insight into the adsorption mechanism of cationic dye onto biosorbents derived from agricultural wastes, *Chem. Eng. Commun.*, 204 (2017) 1020–1036.
- [25] A.C. Martins, O. Pezoti, A.L. Cazetta, K.C. Bedin, D.A.S. Yamazaki, G.F.G. Bandoch, T. Asefa, J.V. Visentainer, V.C. Almeida, Removal of tetracycline by NaOH-activated carbon produced from macadamia nut shells: kinetic and equilibrium studies, *Chem. Eng. J.*, 260 (2015) 291–299.
- [26] S. Wong, Y. Lee, N. Ngadi, I.M. Inuwa, B.M. Nurul Balqis, Synthesis of activated carbon from spent tea leaves for aspirin removal, *Chin. J. Chem. Eng.*, 26 (2018) 1003–1011.
- [27] Z. Hu, H. Chen, F. Ji, S. Yuan, Removal of Congo red from aqueous solution by cattail root, *J. Hazard. Mater.*, 173 (2010) 292–297.
- [28] M.C. Somasekhara Reddy, Removal of direct dye from aqueous solution with a novel adsorbent made from tamarind fruit shell, an agricultural solid waste, *J. Sci. Ind. Res.*, 65 (2006) 443–446.
- [29] S. Venkat, P.V. Vijay Babu, Kinetic and equilibrium studies on the removal of Congo red from aqueous solution using Eucalyptus wood (*Eucalyptus globulus*) sawdust, *J. Taiwan Inst. Chem. Eng.*, 44 (2013) 81–88.
- [30] E. Ghasemian, Z. Palizban, Comparisons of azo dye adsorptions onto activated carbon and silicon carbide nanoparticles loaded on activated carbon, *Int. J. Environ. Sci. Technol.*, 13 (2016) 501–512.
- [31] S. Yadav, A. Asthana, R. Chakraborty, B. Jain, A.K. Singh, S.A.C. Carabineiro, M.A.B. Susan, Cationic dye removal using novel magnetic/activated charcoal/ β -cyclodextrin/alginate polymer nanocomposite, *Nanomaterials (Basel)*, 10 (2020) 170, doi: 10.3390/nano10010170.
- [32] H. Ait Ahsaine, M. Zbair, Z. Anfar, Y. Naciri, R. El Haouti, N. El Alem, M. Ezahri, Cationic dyes adsorption onto high surface area ‘almond shell’ activated carbon: kinetics, equilibrium isotherms, and surface statistical modeling, *Mater. Today Chem.*, 8 (2018) 121–132.